Solar Energy Materials & Solar Cells 103 (2012) 98–107

Contents lists available at SciVerse ScienceDirect

Solar Energy Materials & Solar Cells

journal homepage: www.elsevier.com/locate/solmat

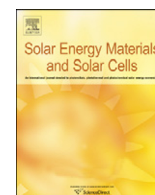

Fabrication of antireflective layers on silicon using metal-assisted chemical etching with in situ deposition of silver nanoparticle catalysts

Xuewen Geng [a,b,**], Zhe Qi [c], Meicheng Li [d], Barrett K. Duan [e], Liancheng Zhao [a], Paul W. Bohn [b,e,*]

[a] School of Materials Science and Engineering, Harbin Institute of Technology, No.92, West Da-Zhi Street, Harbin, Heilongjiang Province 150001, People's Republic of China
[b] Department of Chemical and Biomolecular Engineering, University of Notre Dame, Notre Dame, IN 46556, USA
[c] Institute of Chemistry, Chinese Academy of Sciences, Beijing 100190, People's Republic of China
[d] Renewable Energy School, North China Electric Power University, Beijing 102206, People's Republic of China
[e] Department of Chemistry and Biochemistry, University of Notre Dame, Notre Dame, IN 46556, USA

ARTICLE INFO

Article history:
Received 9 December 2011
Received in revised form
10 April 2012
Accepted 11 April 2012
Available online 8 May 2012

Keywords:
Metal-assisted chemical etching
Antireflection
Porous silicon

ABSTRACT

Ag particle-assisted chemical etching of silicon wafers in HF/H_2O_2 is of interest for its potential to produce antireflective layers for solar cells. In this work, Ag films containing both nanoscale ($d < 100$ nm) and microscale ($d < 1$ μm) particles were deposited through the silver-mirror reaction on planar *p*-Si(111), planar *p*-Si(100) and *p*-Si(100) pre-etched in KOH/isopropanol to produce pyramidal textures. Subsequently, these wafers were subjected to metal-assisted chemical etching (MacEtch) in 1:1:1 (v:v:v) HF(49%):H_2O_2(30%):EtOH solutions, to produce porous silicon (PSi) containing both micro- and nanoscale roughness features. The resulting surfaces exhibit morphologies that evolve with processing conditions, especially the absence/presence of pyramidal textures and the time the structure is subjected to MacEtch. Under optimal conditions excellent anti-reflection behavior is observed with surface reflectivities being reduced below 10% for either *p*-Si(100) or *p*-Si(111) surfaces. For *p*-Si(100) better results ($R \sim 5\%$) were obtained for 30 min KOH/isopropanol pre-etch than for either no pre-etch or longer (60 min) pre-etch. The influence of the reductant on Ag particle deposition on *p*-Si(111) was studied, and MacEtch catalyzed by Ag produced from acetaldehyde reductant produced surfaces with lower reflectivities than those with glucose reductant.

© 2012 Elsevier B.V. All rights reserved.

1. Introduction

Fabrication of antireflective layers on all kinds of silicon surfaces has attracted attention since the 1980s as a key technology to effectively improve the efficiency of silicon solar cells, both in first-generation photovoltaic cells based on bulk materials and second-generation structures based on thin-films [1–15]. Simple, practical methods to texturize silicon surfaces for anti-reflection applications that utilize wet chemical etching are of particular interest, due to their low cost, compatibility with mass production and absence of a residual mechanically damaged layer after etching.

Wet etching approaches can be categorized grossly into alkaline and acidic etches. Alkaline etches are valued for their ability to produce randomly distributed inverted [2,4,14] or upright pyramids [1,3,15] on monocrystalline Si(100) surfaces, based on the fact that different crystallographic planes exhibit different etching rates. These structures can reduce the surface reflectivity drastically in the 400–1200 nm spectral region [3,15], the wavelength band in which most of the energy of the solar spectrum is contained at normal incidence. However, the average reflectivity of these materials remains above 10%, the process must be carried out at elevated temperatures, and sometimes masks are also needed to spatially direct the etching [14]. Acidic etching, typically carried out in $HF/HNO_3/CH_3COOH$ or $HF/HNO_3/H_2O$, is more effective for polycrystalline, rather than monocrystalline, silicon, because it is isotropic [9]. However, the reactions can be difficult to control and can be accompanied by the evolution of undesirable gases, like NO [16,17].

To address some of these processing issues, a novel acid-based oxidation process, termed metal-assisted chemical etching (MacEtch) has been introduced [6,7,10,12,18–21]. MacEtch can be applied to both elemental and compound semiconductors, but it was used initially to prepare porous Si (PSi) from *p*-Si(100) wafers. In MacEtch, noble metal nanoparticles, typically Ag, catalyze the production of holes from chemical oxidants, commonly H_2O_2, which are then injected into the valence band of the semiconductor, resulting in the dissolution of silicon and the formation of etched structures near the particles [19,22]. Many kinds of

* Corresponding author. Tel.: +1 574 631 1849.
** Corresponding author at: School of Materials Science and Engineering, Harbin Institute of Technology, No.92, West Da-Zhi Street, Harbin, Heilongjiang Province 150001, People's Republic of China.
E-mail addresses: gengxuewen@gmail.com (X. Geng), pbohn@nd.edu (P.W. Bohn).

0927-0248/$ - see front matter © 2012 Elsevier B.V. All rights reserved.
http://dx.doi.org/10.1016/j.solmat.2012.04.020

functional nanostructures from 1D to 3D have been fabricated by application of the MacEtch process to silicon using Ag particle catalysts [23,24], with the final etched morphologies being directly related to the characteristics of Ag particles, *e.g.* size, initial spatial distribution, shape etc. For example, quasi-ordered rectangular and hexagonal structures are obtained by Ag-catalyzed MacEtch of *p*-Si(100) and *p*-Si(111), respectively [25]. The initial particle morphology is usually determined by the deposition conditions. Meanwhile, noble metal deposition on silicon has been extensively investigated for applications such as plasmonic coupling of incident radiation into waveguide modes of thin semiconductor photodetectors [26], enhancing layers for surface-enhanced Raman scattering (SERS) [27,28], working electrodes for Faradaic electrochemistry [12] and localizing surface plasmons to enhance the absorbance of silicon solar cells [29]. Thus, the development of Ag particle catalyzed MacEtch to produce practical antireflective layers is of considerable interest.

Here we report a new approach to the production of antireflective materials from crystalline silicon based on the reductive deposition of Ag nanoparticles from solution using the silver-mirror reaction (Tollen's reagent) [30]. Interestingly, after direct deposition of Ag particles on Si surfaces followed by MacEtch, *p*-Si(100) and (111) surfaces are obtained with surface reflectance reduced below 10%. The MacEtch process can also be applied as a second processing step to Si(100) surfaces previously texturized in KOH/IPA, and these structures are compared to those obtained from MacEtch of pristine silicon directly.

2. Experimental section

2.1. Materials

Boron-doped *p*-Si(100) and *p*-Si(111) single crystal wafers with resistivities of $\rho \sim 7–13\ \Omega$ cm and 8–13 Ω cm, respectively, were purchased from Emei Semiconductor Factory, China. Single-polished wafers were cut into $2.0 \times 2.0\ cm^2$ pieces. Deionized (DI) water ($\rho \sim 18.2$ MΩ cm) from a Milli-Q Gradient water purification system (Millipore) was used to prepare all aqueous solutions and for rinsing. All chemicals were used directly as-received, without further purification. Hydrofluoric acid (49% electronic grade) was purchased from Transene Co. Ammonium hydroxide ($NH_3 \cdot H_2O$, 28–30% NH_3, ACS reagent) and sodium hypochlorite solution (NaOCl, 10–15%, reagent grade) were purchased from Sigma-Aldrich Co. Acetaldehyde (CH_3CHO, certified) and hydrogen peroxide (H_2O_2, 30%, certified ACS) were purchased from Fisher Scientific. Silver nitrate ($AgNO_3$, AR), glucose ($CH_2OH(CHOH)_4CHO$, AR), sodium hydroxide (NaOH, AR), potassium hydroxide (KOH, AR), nitric acid (HNO_3, 32–34%, AR), acetone (CH_3COCH_3, AR.CP), isopropyl alcohol (IPA, $(CH_3)_2CHOH$, AR) and ethanol (EtOH) (C_2H_5OH, AR) were purchased from Tianjin Chemical Reagent No. 1 Plant.

2.2. Silver particle deposition

A block diagram describing the processing flow is shown in Fig. S1 in Electronic Supplemental Information (ESI). Before experiments, the glass beakers were cleaned by boiling 10% NaOH solution for 10 min, followed by rinsing with DI water for 5 min (2 times). Ammonium hydroxide was diluted to ~2%, and acetaldehyde was diluted to ~10% using DI water. All singly-polished *p*-Si(100) and Si(111) wafers were pretreated in ~12% aqueous NaOCl for 15 min to remove surface contaminants [8]. Selected *p*-Si(100) wafers were texturized in KOH (1%)/IPA (6v%) at 80 °C for 30 or 60 min. A combination of micro- and nano-sized Ag particles was deposited on the cleaned surfaces of *p*-Si(100) and Si(111) wafers through the silver-mirror reaction after first

Table 1
MacEtch time for *p*-Si wafers.

Samples	S1[a]	S2	S3	S4	S5	S6	S7	S8[b]	S9	S10	S11	S12[b]	S13	S14	S15
***p*-Si(100)**															
Etch *t* (min)	0	10	20	30	60	120	180	0	10	20	30	0	1	5	120
Texturizing conditions	NaOCl							KOH/IPA 30 min no Ag	KOH/IPA 30 min Ag	KOH/IPA 30 min Ag	KOH/IPA 30 min Ag	KOH/IPA 60 min no Ag	KOH/IPA 60 min Ag	KOH/IPA 60 min Ag	KOH/IPA 60 min Ag
Average reflectance	40.7	23.8	11.5	11.5	13.0	14.7	11.0	15.2	9.3	8.6	6.8	18.1	18.1	28.7	5.5
Samples	S16[a]	S17	S18	S19	S20	S21	S22	S23	S24	S25					
***p*-Si(111)**															
Etch *t* (min)	0	10	20	30	120	10	20	30	60	120					
Reductant[c]	NaOCl	Glu	Glu	Glu	Glu	AcA	AcA	AcA	AcA	AcA					
Average reflectance	40.4	15.1	15.5	10.2	9.6	13.6	7.7	6.5	9.1	16.7					

[a] S1 and S16 were processed using NaOCl solution before Ag particle deposition.
[b] S8 and S12 were texturized in KOH/IPA without Ag particle deposition.
[c] Glu = glucose, AcA = acetaldehyde.

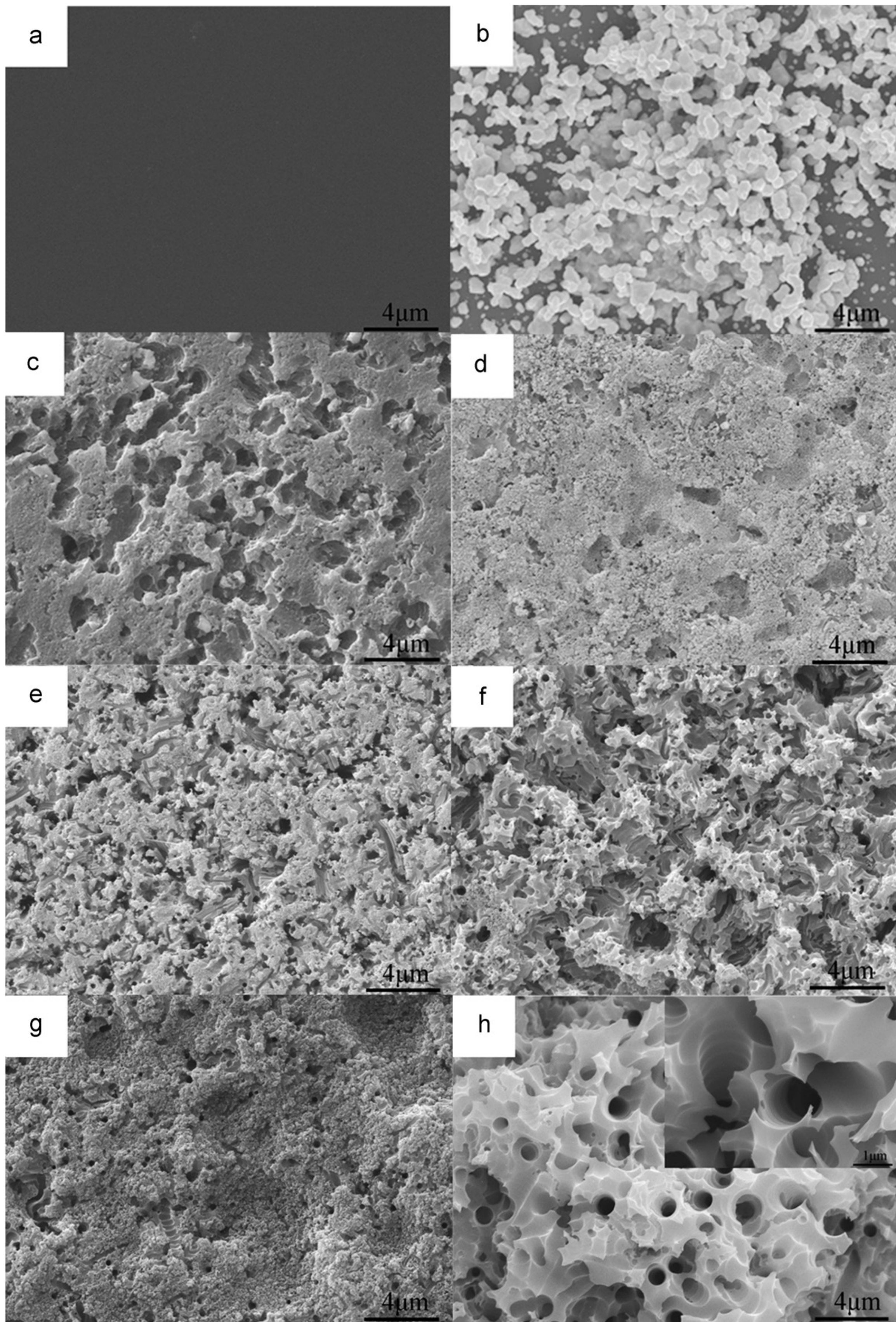

Fig. 1. SEM images of *p*-Si(100) wafers before and after Ag deposition and subsequent MacEtch in 1:1:1 (v:v:v) HF (49%):H_2O_2 (30%):ethanol for varying times. (a) SEM of S1 prior to Ag deposition. (b) SEM of S1 after Ag particle deposition. SEM images after MacEtch for (c) S2, (d) S3, (e) S4, (f) S5, (g) S6, (h) S7, corresponding to 10, 20, 30, 60, 120 and 180 min, respectively. The magnification bar of the inset in (h) is 1 μm.

removing the native SiO_2 from the Si surfaces using dilute HF. To implement the silver-mirror reaction, 2% $NH_3 \cdot H_2O$ was first added dropwise into a 2% $AgNO_3$ solution with stirring to prepare ammoniacal silver nitrate. After immersing the silicon target surfaces, 6% glucose or 10% acetaldehyde solution was slowly added dropwise into the ammoniacal silver nitrate solution, after which the solution was heated to 65 °C. After a short induction period, an Ag film was formed on the wafer surfaces in several minutes.

2.3. MacEtch process

The Ag-decorated Si wafers were then subjected to the MacEtch process in 1:1:1 (v:v:v) HF (49%):H_2O_2 (30%):EtOH for the desired time. Table 1 shows the different MacEtch times and conditions for *p*-Si(100) and Si(111) wafers, as well as the conditions used to prepare the Ag catalysts. All samples were processed at 300K. After etching, samples were removed from the etch bath and then dipped in ~33% aqueous HNO_3 for 30 min to remove any residual Ag particles.

2.4. Characterization

Morphologies of the silver particles and the etched samples were characterized with a thermionic-field emission scanning electron microscope (SEM; Camscam, MX2600). Reflectance spectra were recorded from 300 nm to 800 nm with a UV–vis spectrophotometer (PerkinElmer, Lambda 950) equipped with an integrating sphere. Static water contact angles were measured on the original silicon surfaces and the etched samples under ambient conditions using 4 μL sessile drops with a G10 Drop Shape Analysis System (Krüss, Hamburg, Germany) and calculated using Data Physics Series Contact Angle Analyzer Software.

3. Results and discussion

3.1. Ag-catalyzed MacEtch of p-Si(100)

For silver deposition on all *p*-Si(100) wafers, glucose was used exclusively as the reductant in the silver-mirror reaction. Typically broad distributions of particle sizes are obtained using glucose reductant, and the behavior for both unetched *p*-Si(100) and base-etched *p*-Si(100) presenting pyramidal features is addressed below.

3.1.1. Untreated p-Si(100)

The initial series of samples investigated was comprised of untreated *p*-Si(100) subjected to MacEtch in 1:1:1 (v:v:v) HF (49%):H_2O_2 (30%):ethanol for varying times from 10–180 min. After aqueous NaOCl rinsing, untreated (flat) *p*-Si(100) wafers were processed as described in Fig. S1(a). Fig. 1(b) shows SEM images of the deposited Ag particles on *p*-Si(100). Deposition of Ag films on these Si(100) surfaces is quite facile via the silver-mirror reaction, typically producing fully active films within 1 min. The Ag particles distribute in an open network with sizes ranging from several tens to several hundred nanometers. In the initial stages of silicon MacEtch, the reaction proceeds vigorously with a great deal of gas bubble evolution, causing the Ag particles and clusters to move laterally as they begin to descend into the substrate, leading to the formation of a layer with large-scale roughness features and irregular pores at 10 min etch time, as shown in Fig. 1(c). At 20 min etch time, the top macroporous layer begins to peel off, revealing a thin nanoporous layer, Fig. 1(d), which grows into a deep microporous layer, like that shown in Fig. 1(e), at 30 min etch time.

After the initial vigorous stage of etching, the mechanical disturbance associated with bubble formation abates, and the remaining Ag particles reside within physically separated regions, essentially nascent nanopores. The reflectivity of samples before and after initiating the MacEtch, shown in Fig. 2, follows the same trend as the variation in morphology. After a short etch time, $t < 30$ min, the reflectivity decreases to a stable average reflectivity in the range 300–800 nm of approximately $R_{avg} \sim 10\%$, where it remains, even for prolonged etch times, as shown in Fig. 2(b). Fig. 1(e)–(h) shows that the morphology of the etched Si continues to evolve over etch times in the range 30–180 min, but the reflectivity does not change significantly after 30 min. Fig. 1(h) shows the morphology of a *p*-Si(100) sample subjected to MacEtch for 3 h. The formation of a stable microporous layer is evident, and the inset image shows the formation of steps on the sidewalls of the nanopores. Although the stepped features do not correlate with further decreases in reflectance under these conditions, they are a characteristic feature of MacEtch in silicon, and they do appear to correlate with further reductions in reflectance under other conditions (*vide infra*).

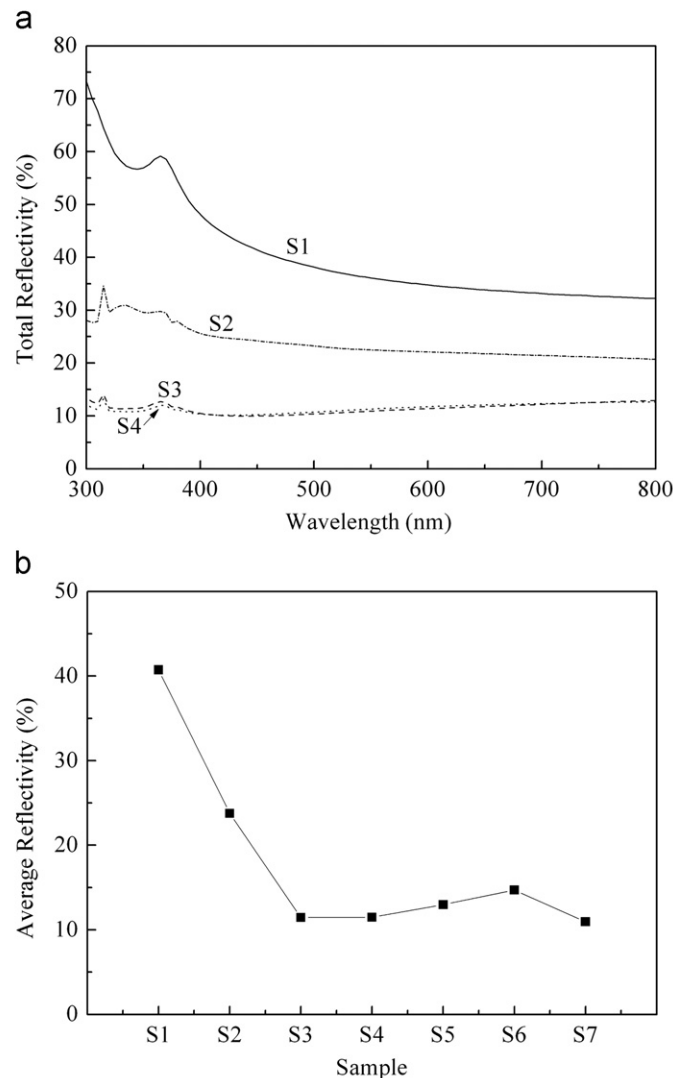

Fig. 2. Reflectivity of *p*-Si(100) samples before and after MacEtch for various etching times. (a) Reflectance spectra of samples etched for various times (0, 10, 20 and 30 min); (b) Variation of average reflectivity (300–800 nm) for samples etched varying times (0, 10, 20, 30, 60, 120, 180 min).

3.1.2. Effect of KOH pre-etching on MacEtch of p-Si(100)

One hypothesis posits that the presence of nano- and micro-scale roughness features in the same sample structure can aid in achieving low-reflectance surfaces. In order to test this hypothesis, a two-stage processing strategy was developed in which a first stage etch in KOH/isopropanol (IPA) is used to produce μm-scale pyramidal features in the (100) geometry, and this is followed by Ag-catalyzed MacEtch to produce nanoscale features on the μm-scale pyramids. The process followed is shown in the flow chart in Fig. S1(b) in the ESI. The first stage etch was implemented for either 30 min (S8-S11) or 60 min (S12-S15) to produce two series of samples.

Fig. 3 shows the results for samples etched 30 min in hot KOH/IPA, including the micro-pyramids obtained in the first stage etch, Fig. 3(a), the morphology of the deposited Ag particles, Fig. 3(b), and the corresponding morphologies obtained at various MacEtch times. Starting from uniformly distributed pyramids of average size ~1 μm produced by 30 min exposure to KOH/IPA at 80 °C, Ag particles or clusters obtained from Tollen's reagent distributed on the surface similarly to those on unetched Si, Fig. 1(b), except for the preferential deposition of Ag along the bases of the pyramids. Note the square features in Fig. 3(b). The morphologies obtained from 10–30 min MacEtch are shown in Fig. 3(c)–(e). Unlike the results obtained from MacEtch of *n*-Si(100) using Ag particles deposited by chemical replacement [31], no hierarchical structures are observed. Instead, porous layers are obtained, in which the porosity evolves with etch time. Interestingly, as shown in Fig. S2, these samples all show lower reflectivity than either (a)

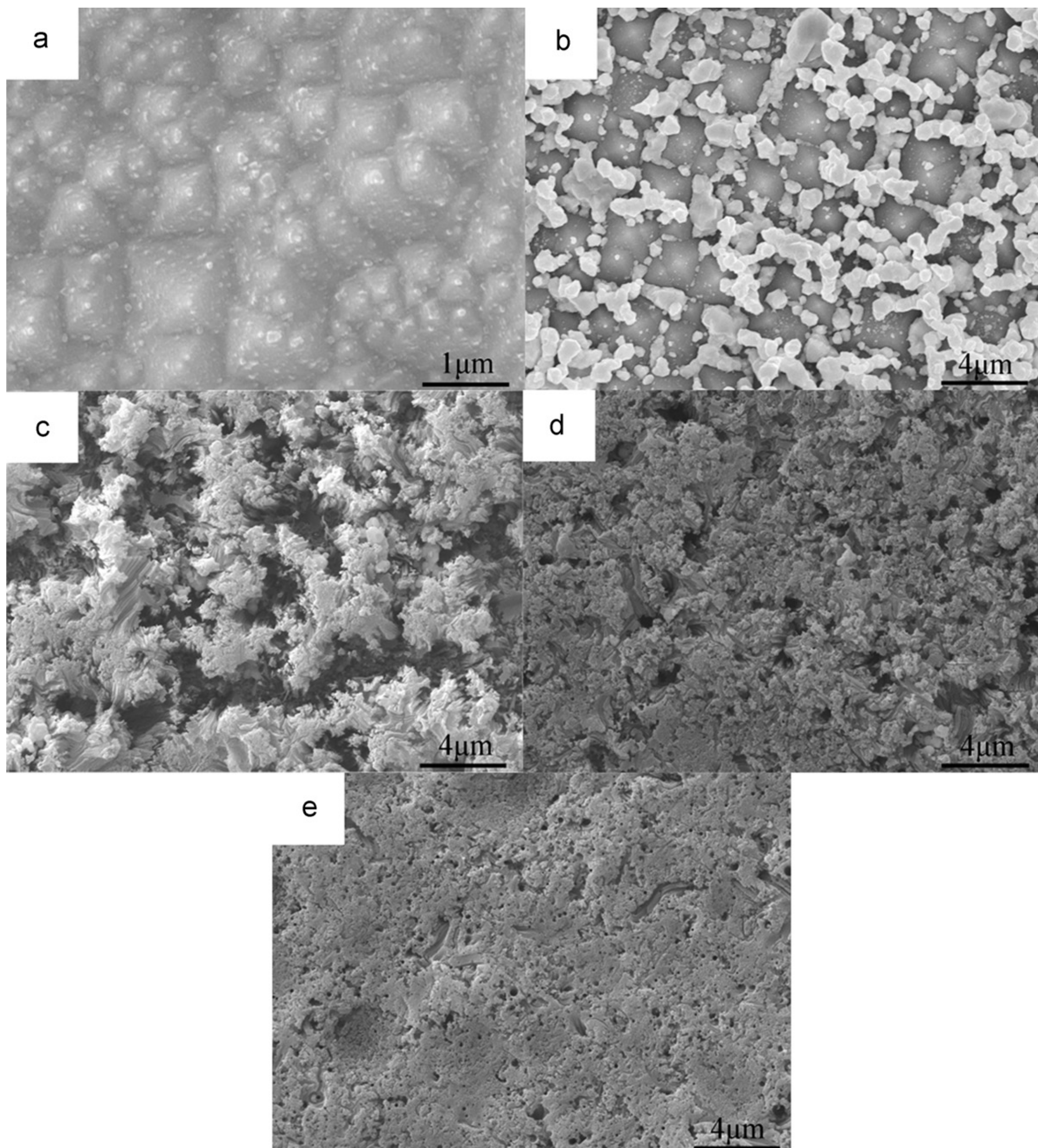

Fig. 3. SEM images of *p*-Si(100) wafers before and after Ag particle deposition on surfaces pre-etched to produce a random pyramidal texture and subsequent MacEtch in 1:1:1 (v:v:v) HF (49%):H_2O_2 (30%):ethanol for varying times. (a) SEM of S8 prior to Ag deposition. (b) SEM of S8 after Ag particle deposition. SEM images after MacEtch on samples (c) S9, (d) S10, (e) S11, etched for 10, 20 and 30 min, respectively.

the pyramidal textures not subjected to MacEtch or (b) surfaces produced from MacEtch of flat silicon. Furthermore, the average reflectivity in the range 300–800 nm is reduced below 10%, which is a threshold for potential application as antireflection layers of solar cells.

Fig. 4 shows the results for *p*-Si(100) samples etched 60 min in hot KOH/IPA, including the micro-pyramids obtained in the first stage etch, Fig. 4(a), the morphology of the deposited Ag particles, Fig. 4(b), and the corresponding morphologies obtained at various MacEtch times, Fig. 4(d)–(f). Fig. 4(a) shows that the surface morphology of the Si(100) micro-textured with pyramids in KOH/IPA at 80 °C for 60 min is less uniform in size than comparable samples exposed to KOH/IPA for 30 min. Correspondingly, the surface reflectivity prior to MacEtch is significantly larger, as shown in Fig. S3. These rougher structures apparently facilitate the nucleation and deposition of Ag particles, as the Ag layer obtained under the same conditions applied in Fig. 3(b) is much thicker and denser, as shown in Fig. 4(b). This surface exhibits roughness over a large span of length scales, as supported by the superhydrophobic behavior in a sessile drop water contact angle measurement, Fig. 4(c). Consistent with the larger Ag loading, the MacEtch reaction initially proceeds very rapidly, and the resulting mechanical disturbance causes the pyramidal textures to collapse within 1 min, replacing the pyramidal architecture with an uneven microporous layer, as shown in Fig. 4(d). The surface morphology continues to evolve in a complex fashion at longer MacEtch times (not shown) with relatively high average reflectance values (Table 1). In contrast, very long MacEtch times ($t \sim 120$ min) result in a distinctly different morphology exhibiting large-area disordered bunched nanowire-like structures,

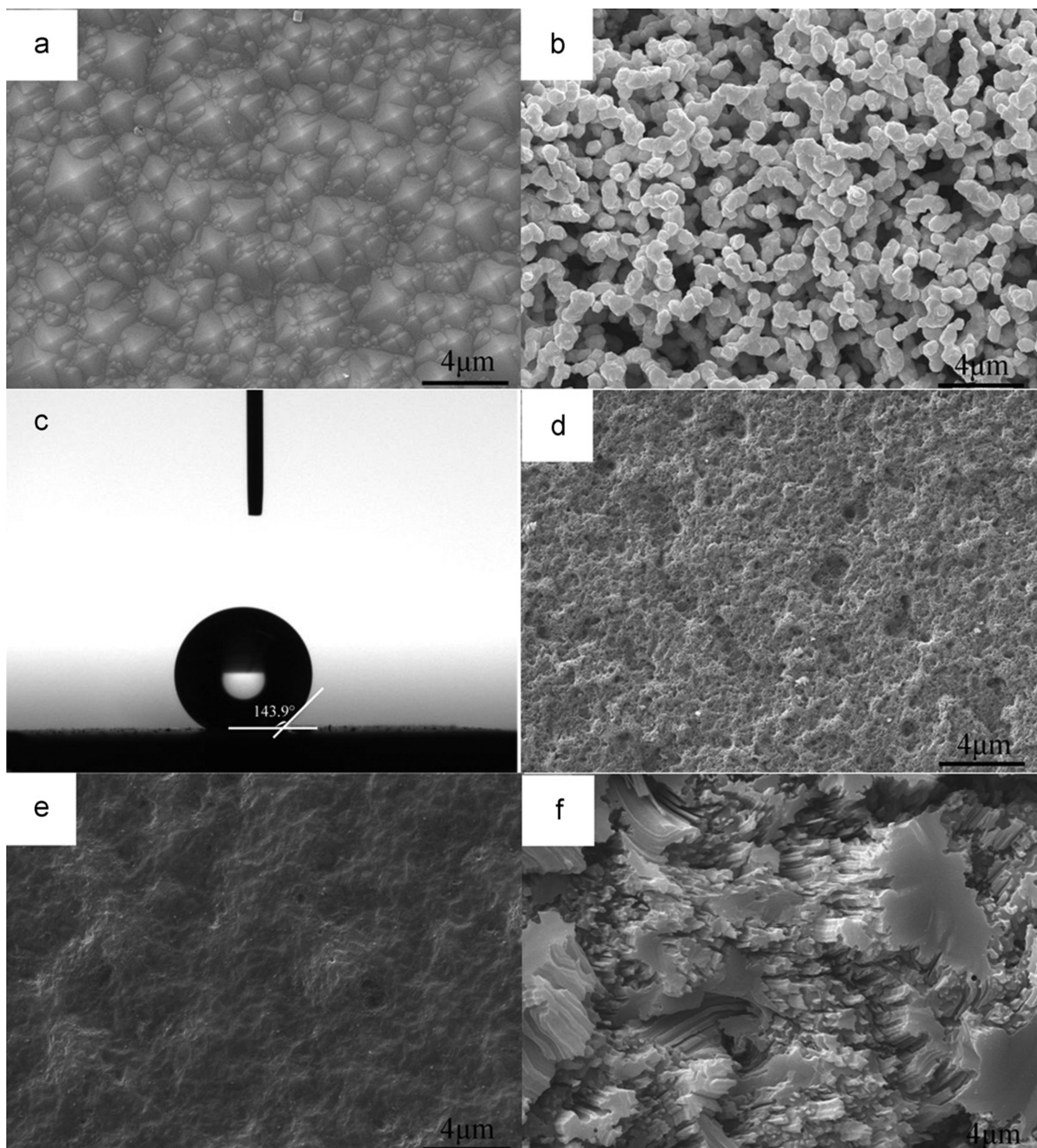

Fig. 4. Behavior of *p*-Si(100) wafers before and after Ag particle deposition on surfaces pre-etched to produce a random pyramidal texture and subsequent MacEtch in 1:1:1 (v:v:v) HF (49%):H_2O_2 (30%):ethanol for varying times. (a) SEM of S12 prior to Ag deposition. (b) SEM S12 after Ag particle deposition. (c) Sessile drop water contact angle on sample in panel (b). SEM images after MacEtch on samples (d) S13, (e) S14, (f) S15, subjected to MacEtch for 1, 5 and 120 min, respectively.

as shown in Fig. 4(f). Importantly, these structures display average reflectance $R_{avg}\sim 5\%$—as good as the best results obtained under any of the etching protocols examined here. Table 1 summarizes the average reflectance results for all of the pre-etched *p*-Si(100) samples. It is evident that the two-step etching strategy is effective under carefully controlled conditions in producing samples with lower reflectivity than either the KOH/IPA-produced pyramidal textures or the flat *p*-Si(100) subjected to MacEtch only.

3.2. Ag-catalyzed MacEtch of p-Si(111)

To investigate the effect of crystalline facet, a series of experiments were performed on *p*-Si(111), using two reductants, glucose and acetaldehyde, which produce distinct Ag catalyst morphologies. After aqueous NaOCl rinsing, flat *p*-Si(111) wafers were processed in the sequences represented in Fig. S1(b).

3.2.1. MacEtch of p-Si(111) with glucose-reduced Ag particles

Typically an alkaline environment is required to ensure the deposition of metal films by the silver-mirror reaction. Here two different reducing agents with different reduction potentials, glucose and acetaldehyde, are compared for their ability to facilitate the formation of Ag particles, which can then catalyze the MacEtch process. Fig. 5 shows SEM images of *p*-Si(111) wafers before and after Ag particle deposition, using glucose as reductant, and subsequent MacEtch in 1:1:1 (v:v:v) HF (49%):H_2O_2 (30%):ethanol for different times. The Ag particles produced by the silver-mirror reaction in 1 min under these conditions display sizes ranging from

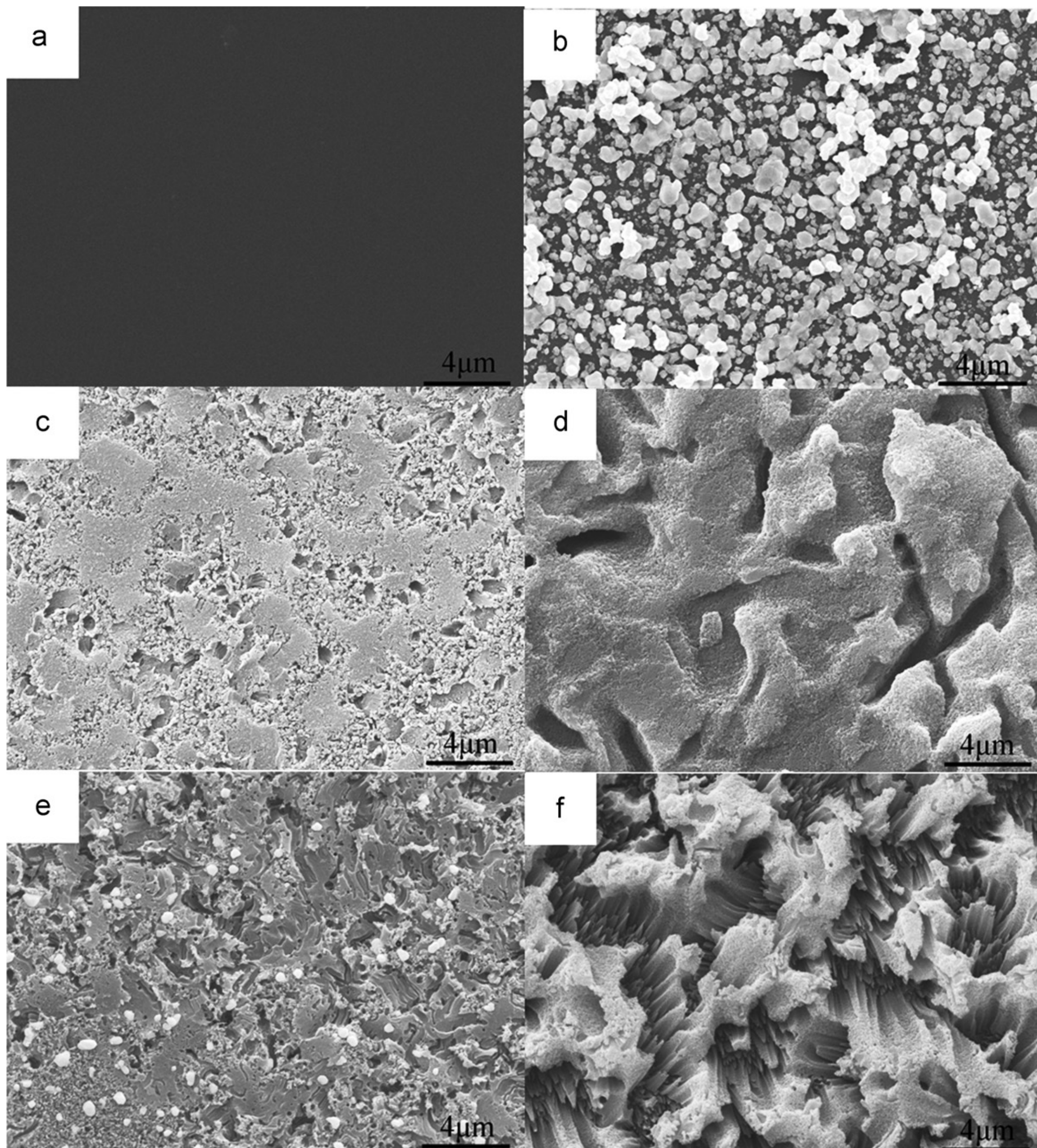

Fig. 5. SEM images of *p*-Si(111) wafers before and after Ag particle deposition, using glucose as reductant, and subsequent MacEtch in 1:1:1 (v:v:v) HF (49%):H_2O_2 (30%):ethanol for different times. (a) S16 prior to processing. (b) S16 after Ag particle deposition. SEM images after etching for (c) S17, (d) S18, (e) S19, (f) S20, which are etched for 10, 20, 30 and 120 min, respectively.

several tens to several hundred nanometers distributed randomly as shown in Fig. 5(b), however both the density of Ag particles and the thickness of the Ag film are much smaller than those produced on *p*-Si(100) surfaces. Fig. 5(c) shows a non-uniform morphology – slightly etched micro-domains surrounded by nanopores – after a 10 min MacEtch. Even at this short etch duration the reflectance spectrum, Fig. S4, still shows much lower reflectivity than the polished wafer and the average reflectivity in 300–800 nm is reduced to about 15%. When increasing the MacEtch time to 20 and 30 min, viz. Fig. 5(d) and (e), the small porous domains grow into bigger grooves and the surface becomes more uneven, ultimately evolving into the bunched wire-like structures appeared, as shown in Fig. 5(f) at 120 min etch time. After dropping significantly during the first 10 min etch period the average reflectance stabilizes near $R_{avg}\sim 10\%$ at all longer etch times. The uniformity of structures produced by this method can be controlled by adjusting the experimental conditions affecting etch rates, Fig. S5. MacEtch using metals deposited by sputtering or evaporation produces etch rates sufficiently fast that control of uniformity is difficult to achieve. For MacEtch using in situ deposition, the etching process is affected by the initial conditions, including the crystal orientation, cleanliness degree. However, the uniformity and the density of the deposited particles and even the diameter of the particles can be controlled by adjusting the solution concentration and the deposition temperature, and the etch rate can be controlled by adjusting the concentrations of the etchants.

3.2.2. MacEtch of *p*-Si(111) with acetaldehyde-reduced Ag particles

When acetaldehyde is used as the reductant in the silver-mirror reaction deposition of Ag on *p*-Si(111), the induction

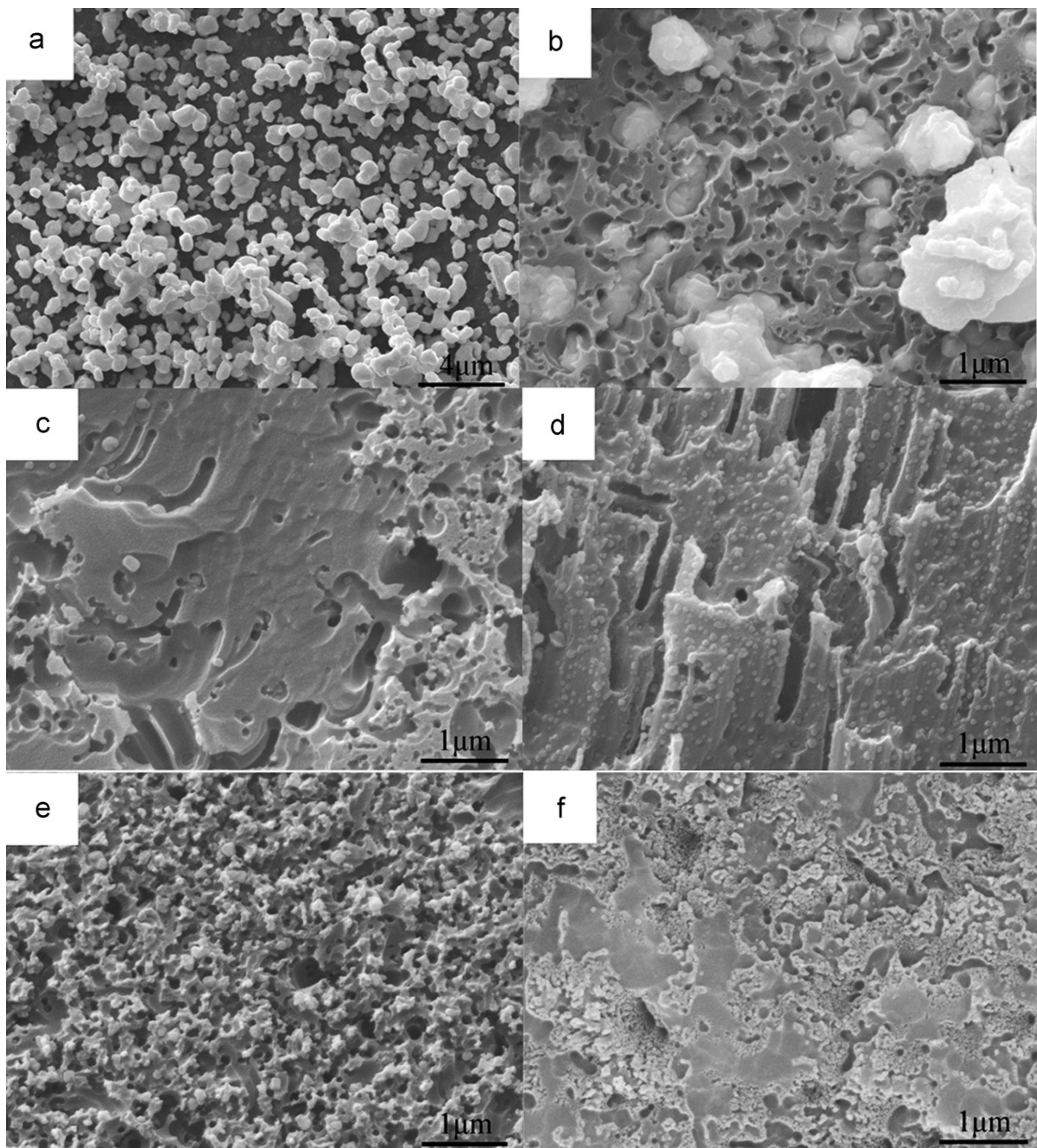

Fig. 6. SEM images of *p*-Si(111) wafers after Ag particle deposition, using acetaldehyde as reductant, and subsequent MacEtch in 1:1:1 (v:v:v) HF (49%):H_2O_2 (30%): ethanol for different times. (a) S16 after Ag deposition but prior to etching. SEM images after etching for (b) S16, (c) S21, (d) S22, (e) S23, and (f) S25, which are etched for 0, 10, 20, 30, 60, 120. Note the scale bar is 1 μm for panels (b)–(f).

period is much longer than when glucose is used, consistent with the fact that acetaldehyde is a less active reducing agent than glucose. Furthermore, Fig. 6(a) shows the Ag particle size distribution is much more homogeneous than that obtained with glucose, Fig. 5(b). Fig. 6(c)–(f) show the results of MacEtch carried out for varying times with these Ag deposits, and Fig. S6 shows the measured reflectance spectra and average reflectances. The observed morphology changes are similar to those obtained with the glucose-derived Ag catalyst, with the exception that very long etches do not produce the wire-like morphology observed in sample S20 ($t=120$ min). Importantly, low average reflectivities are obtained over a broad range of etch times, as shown in Fig. S6(b) and Table 1, being below 10% average reflectivity over the range 20 min $< t <$ 60 min. This observation is correlated with the homogeneity of the Ag particle size distribution using acetaldehyde as the reductant, and the average reflectance values obtained are as low as the best structures prepared from the two-stage micro-nano etch strategy used with *p*-Si(100). They are certainly low enough to be of technological interest, especially given the simplicity of the preparation process.

4. Conclusion

Antireflective porous layers can be fabricated in a simple straightforward liquid-phase process on *p*-Si(100) and (111) by Ag-catalyzed MacEtch in 1:1:1 (v:v:v) HF(49%):H_2O_2(30%):ethanol at ambient temperature. The catalyst Ag particles are deposited via the silver-mirror reaction by using either glucose or acetaldehyde as reductant, and in the case of *p*-Si(100), the surfaces can be pre-etched in KOH/IPA to produce pyramidal structures prior to MacEtch. Processing schemes producing reflectance values below 10% averaged over the wavelength range 300–800 nm are promising for technological application. The best results, *i.e.* lowest average reflectance values, are obtained with the two-step etching strategy applied to *p*-Si(100). A 30 min KOH/IPA pre-etch coupled with relatively short MacEtch times ($t<30$ min) produces samples with surface reflectivities ~5%. These results are better than those obtained with pyramidal textures alone or the MacEtch of flat *p*-Si(100). Low reflectivity structures can also be produced from *p*-Si(111) surfaces using Ag catalysts derived either from glucose or acetaldehyde reductants, with average reflectivities $\leq 10\%$. Slightly better results are obtained using acetaldehyde, $R_{avg} < 10\%$, in a process that is relatively insensitive to the MacEtch time employed. In summary, the novel method described here offers a simple route to the production of antireflective layers directly on *p*-Si(100) and (111) surfaces and can likely be extended to antireflection coatings on polycrystalline wafers.

Acknowledgments

This work was supported by the Program for New Century Excellent Talents in University of China (NCET-06-0337), the US National Science Foundation grant NSF CHE-1111739 and by the Army Corps of Engineers through contract W9132T-07-2-0003.

Appendix A. Supporting information

Supplementary data associated with this article can be found in the online version at http://dx.doi.org/10.1016/j.solmat.2012.04.020.

References

[1] P. Campbell, M.A. Green, Light trapping properties of pyramidally textured surfaces, Journal of Applied Physics 62 (1987) 243–249.
[2] T. Hantschel, W. Vandervorst, Anisotropic etching of inverted pyramids in the sub-100 nm region, Microelectronic Engineering 35 (1997) 405–407.
[3] E. Vazsonyi, K. De Clercq, R. Einhaus, E. Van Kerschaver, K. Said, J. Poortmans, J. Szlufcik, J. Nijs, Improved anisotropic etching process for industrial texturing of silicon solar cells, Solar Energy Materials and Solar Cells 57 (1999) 179–188.
[4] A.W. Smith, A. Rohatgi, Ray tracing analysis of the inverted pyramid texturing geometry for high-efficiency silicon solar-cells, Solar Energy Materials and Solar Cells 29 (1993) 37–49.
[5] H. Nagayoshi, K. Konno, S. Nishimura, K. Terashima, Surface texturing of silicon by hydrogen radicals, Japanese Journal of Applied Physics 44 (2005) 7839–7842.
[6] K.Q. Peng, M.L. Zhang, A.J. Lu, N.B. Wong, R.Q. Zhang, S.T. Lee, Ordered silicon nanowire arrays via nanosphere lithography and metal-induced etching, Applied Physics Letters 90 (2007) 163123-1–163123-3.
[7] S. Koynov, M.S. Brandt, M. Stutzmann, Black nonreflecting silicon surfaces for solar cells, Applied Physics Letters 88 (2006) 203107-1–203107-3.
[8] U. Gangopadhyay, S.K. Dhungel, A.K. Mondal, H. Saha, J. Yi, Novel low-cost approach for removal of surface contamination before texturization of commercial monocrystalline silicon solar cells, Solar Energy Materials and Solar Cells 91 (2007) 1147–1151.
[9] Y. Kim, S.K. Dhungel, S. Jung, D. Mangalaraj, J. Yi, Texturing of large area multi-crystalline silicon wafers through different chemical approaches for solar cell fabrication, Solar Energy Materails and Solar Cells 92 (2008) 960–968.
[10] H. Fang, X.D. Li, S. Song, Y. Xu, J. Zhu, Fabrication of slantingly-aligned silicon nanowire arrays for solar cell applications, Nanotechnology 19 (2008) 255703-1–255703-6.
[11] T. Sato, T. Sugiura, M. Ohtsubo, S. Matsuno, M. Konagai, Texture etching of Si with atomic hydrogen generated by hot wire method through SiO_2 masks for solar cell applications, Japanese Journal of Applied Physics 46 (2007) 6796–6800.
[12] K. Tsujjino, M. Matsumura, Formation of a low reflective surface on crystalline silicon solar cells by chemical treatment using Ag electrodes as the catalyst, Solar Energy Materials and Solar Cells 90 (2006) 1527–1532.
[13] M. Moreno, D. Daineka, P.R.I. Cabarrocas, Plasma texturing for silicon solar cells: From pyramids to inverted pyramids-like structures, Solar Energy Materials and Solar Cells 94 (2010) 733–737.
[14] J.S. You, D. Kim, J.Y. Huh, H.J. Park, J.J. Pak, C.S. Kang, Experiments on anisotropic etching of Si in TMAH, Solar Energy Materials and Solar Cells 66 (2001) 37–44.
[15] Y. Nishimoto, K. Namba, Investigation of texturization for crystalline silicon solar cells with sodium carbonate solutions, Solar Energy Materials and Solar Cells 61 (2000) 393–402.
[16] W.C. Hui, How to prevent a runaway chemical reaction in the isotropic etching of silicon with $HF/HNO_3/CH_3COOH$ or HNA solution, in: J.-C. Chiao, A.J. Hariz, D.N. Jamieson, G. Parish, V.K. Varadan (Eds.), Device and Process Technologies for MEMS, Microelectronics, and Photonics III, Proceedings of the SPIE 5276, 2004, pp. 270–276.
[17] M. Steinert, J. Acker, A. Henssge, K. Wetzig, Experimental studies on the mechanism of wet chemical etching of silicon in HF/HNO_3 mixtures, Journal of the Electrochemical Society 152 (2005) C843–C850.
[18] C. Chartier, S. Bastide, C. Levy-Clement, Metal-assisted chemical etching of silicon in $HF–H_2O_2$, Electrochimica Acta 53 (2008) 5509–5516.
[19] S. Chattopadhyay, X.L. Li, P.W. Bohn, In-plane control of morphology a nd tunable photoluminescence in porous silicon produced by metal-assisted electroless chemical etching, Journal of Applied Physics 91 (2002) 6134–6140.
[20] W. Chern, K. Hsu, I.S. Chun, B.P. de Azeredo, N. Ahmed, K.H. Kim, J.M. Zuo, N. Fang, P. Ferreira, X.L. Li, Nonlithographic patterning and metal-assisted chemical etching for manufacturing of tunable light-emitting silicon nanowire arrays, Nano Letters 10 (2010) 1582–1588.
[21] W.Q. Xie, J.I. Oh, W.Z. Shen, Realization of effective light trapping and omnidirectional antireflection in smooth surface silicon nanowire arrays, Nanotechnology 22 (2011) 065704-1–065704-9.
[22] X. Li, P.W. Bohn, Metal-assisted chemical etching in HF/H_2O_2 produces porous silicon, Applied Physics Letters 77 (2000) 2572–2574.
[23] T. Qiu, P.K. Chu, Self-selective electroless plating: An approach for fabrication of functional 1D nanomaterials, Materials Science and Engineering R-Reports 61 (2008) 59–77.
[24] O.J. Hildreth, W. Lin, C.P. Wong, Effect of catalyst shape and etchant composition on etching direction in metal-assisted chemical etching of silicon to fabricate 3D nanostructures, ACS Nano 3 (2009) 4033–4042.
[25] X. Geng, M. Li, L. Zhao, P. Bohn, Metal-assisted chemical etching using Tollen's reagent to deposit silver nanoparticle catalysts for fabrication of quasi-ordered silicon micro/nanostructures, Journal of Electronic Materials 40 (2011) 2480–2485.
[26] H.R. Stuart, D.G. Hall, Absorption enhancement in silicon-on-insulator waveguides using metal island films, Applied Physics Letters 69 (1996) 2327–2329.
[27] W.C. Ye, C.M. Shen, J.F. Tian, C.M. Wang, L.H. Bao, H.J. Gao, Self-assembled synthesis of SERS-active silver dendrites and photoluminescence properties of a thin porous silicon layer, Electrochemistry Communications 10 (2008) 625–629.

[28] W.C. Ye, C.M. Shen, J.F. Tian, C.M. Wang, C. Hui, H.J. Gao, Controllable growth of silver nanostructures by a simple replacement reaction and their SERS studies, Solid State Sciences 11 (2009) 1088–1093.
[29] S. Pillai, K.R. Catchpole, T. Trupke, M.A. Green, Surface plasmon enhanced silicon solar cells, Journal of Applied Physics 101 (2007) 093105-1–093105-8.
[30] S. Siggia, E. Segal, Determination of aldehydes in the presence of acids, ketones, acetals, and vinyl ethers, Analytical Chemistry 25 (1953) 640–642.
[31] D.A.P. Qi, N. Lu, H.B. Xu, B.J. Yang, C.Y. Huang, M.J. Xu, L.G. Gao, Z.X. Wang, L.F. Chi, Simple approach to wafer-scale self-cleaning antireflective silicon surfaces, Langmuir : The ACS Journal of Surfaces and Colloids 25 (2009) 7769–7772.